

Excitation and relaxation energies of *trans*-stilbene: Confined singlet, triplet, and charged bipolarons

Z. G. Soos

Department of Chemistry, Princeton University, Princeton, New Jersey 08544

S. Ramasesha

*Department of Chemistry, Princeton University, Princeton, New Jersey 08544
and Solid State and Structural Chemistry Unit, Indian Institute of Science, Bangalore 560012, India*

D. S. Galvão

*Bell Communications Research, Red Bank, New Jersey 07701
and Departamento de Física Aplicada, Universidade Estadual de Campinas, 13081 Campinas, São Paulo, Brazil*

S. Etemad

Bell Communications Research, Red Bank, New Jersey 07701

(Received 31 July 1992)

The π -electronic excitations and excited-state geometries of *trans*-stilbene (tS) are found by combining exact solutions of the Pariser-Parr-Pople (PPP) model and semiempirical Parametric Method 3 (PM3) calculations. Comprehensive comparisons with tS spectra are obtained and related to the fluorescence and topological alternation of poly(paraphenylenevinylene) (PPV). The one-photon absorption and triplet of tS correspond, respectively, to singlet and triplet bipolarons confined to two phenyls, while the tS^{2-} ground state is a confined charged bipolaron. Independent estimates of the relaxation energy between vertical and adiabatic excitation show the bipolaron binding energy to depend on both charge and spin, as expected for interacting π electrons in correlated or molecular states. Complete configuration interaction within the PPP model of tS accounts for the singlet-triplet gap, for the fine-structure constants and triplet-triplet spectra, for two-photon transitions and intensities, and for one-photon spectra and the radiative lifetime, although the relative position of nearly degenerate covalent and ionic singlets is not resolved. The planar PM3 geometry and low rotational barrier of tS agree with resolved rotational and vibrational spectra in molecular beams. PM3 excitation and relaxation energies for tS bipolarons are consistent with experiment and with PPP results. Instead of the exciton model, we interpret tS excitations in terms of states that are localized on each ring or extended over an alternating chain, as found exactly in Hückel theory, and find nearly degenerate transitions between extended and localized states in the singlet, triplet, and dianion manifolds. The large topological alternation of the extended system increases the ionicity and interchanges the order of the lowest one- and two-photon absorption of PPV relative to polyenes.

I. INTRODUCTION

The *cis-trans* isomerization of stilbene has been of enduring interest, with events on the fs timescale now accessible.¹ The electronic states of *trans*-stilbene (tS) have also been extensively studied, both experimentally and theoretically, since Dyck and McClure's classic absorption and fluorescence study.² The ground (S_0) and excited (S_1) potential surfaces, for example, have been obtained by Negri, Orlandi, and Zerbetto³ in terms of the QCFF/PI model of Warshel and Karplus,⁴ in which a force field for σ electrons is combined with a Pariser-Parr-Pople (PPP) model for the π electrons. The results account well for the resolved rotational structure of tS reported subsequently by Champagne *et al.*⁵

Several aspects of the electronic structure of tS are illustrated by this example. First, modern quantum-chemical methods for molecular structure are combined with a PPP description of low-lying excitations. We will

use the recent⁶ Parametric Method 3 (PM3) to probe the ground- and excited-state geometries of tS and will present exact PPP rather than limited configuration-interaction (CI) results, thereby obtaining the most comprehensive assignment to date for singlet and triplet excited states. Second, high accuracy for the S_0 - S_1 splitting⁵ leaves open the ordering or nature of the low-lying states. The relative ordering of S_1 and two-photon states reported by Hohlneicher and Dick⁷ are particularly challenging. As summarized recently by Lhost and Brédas,⁸ the planarity of tS is complicated by essentially free rotation about single bonds. Detailed structural and electronic investigations of tS thus coexist with apparently simple, but basic questions.

We focus in this paper on the electronic and structural properties of tS, of its low-lying excited states, and of its ions. Molecular information about tS or tS^{2-} bears⁹ directly on the electronic structure of poly(paraphenylenevinylene) (PPV), whose strong fluores-

cence¹⁰ has opened new possibilities for conjugated polymers. In that context, the tS states S_1 and T_1 are, respectively, singlet and triplet bipolarons confined to two phenyls, while the dianion corresponds to the charged bipolaron. A joint structural and electronic study of tS provides accurate experimental information about confined bipolarons.

The Su-Schrieffer-Heeger (SSH) model¹¹ describes the formation of self-localized states in conjugated polymers due to linear electron-phonon (e -ph) coupling and has been widely used^{12,13} to interpret photoinduced or dopant-induced spectra. Since delocalized π electrons do not interact in Hückel or SSH theory, the binding energies of singlet, triplet, or charged bipolarons are all equal, but are not readily measurable. The need to include Coulomb interactions among π electrons motivated the development of the PPP model^{14,15} for conjugated molecules, and the need for electron-electron (e - e) correlations¹⁶ extends to conjugated polymers. We find the binding energies of tS bipolarons to depend on both spin and charge, thereby supporting a more correlated or excitonic¹⁷ description of PPV.

Another motivation for the present work is to compare and contrast the very different computational approaches of PM3 and PPP. All valence electrons are kept in PM3 and an optimized geometry is obtained via a self-consistent-field (SCF) calculation,⁶ thus including average e - e interactions. Quite typically of quantum-chemical methods, the ground-state potential is sought for a single-determinantal function, without CI. The PPP model, by contrast, is restricted to π electrons for a given molecular geometry and the extent of CI is critical for excitation energies. We obtain the first exact, or complete CI, PPP results for tS by using diagrammatic valence-bond (DVB) methods.¹⁸

We begin in Sec. II with PM3 results for the geometry of tS, its excited states, and its ions, and compare the barrier for single-bond rotation with other calculations and with resolved vibrational spectra. Exact PPP results are presented in Sec. III for planar tS with standard molecular parameters and related to one- and two-photon spectra, to triplet-state properties, and to tS^{2-} spectra. The PM3 geometries are compared in Sec. IV with PPP bond orders and relaxation energies for excited states are estimated using PPP, PM3, and combined results. We then discuss the surprisingly consistent PM3 and PPP picture of tS bipolarons, their relation to PPV, and the topological implications of *para*-conjugated phenyl rings on the effective alternation and the relative positions of one- and two-photon excitations.

II. PM3 GEOMETRY OF tS, EXCITED STATES, AND IONS

A. Ground-state geometry

The idealized tS geometry in Fig. 1(a) is planar, with 120° bond angles, benzene bond lengths of $R_0 = 1.397$ Å, and partial single and double bonds of 1.45 and 1.35 Å. There is an inversion center in the double bond and the numbering in Fig. 1(a) is used throughout the paper. The

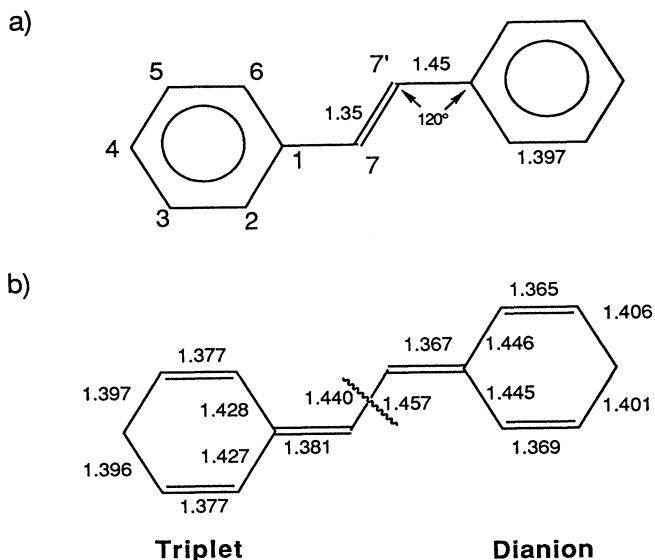


FIG. 1. (a) Idealized ground-state geometry of *trans*-stilbene; (b) PM3 bond lengths of the triplet excited state and the tS^{2-} ground state.

ground- and excited-state geometries of tS deviate from Fig. 1(a) as discussed below.

PM3 is a semiempirical, all-valence-electron method designed to balance reliable geometries and computational effort.⁶ Although motivated as an improvement to AM1, that is still a matter for debate.¹⁹ The improvement of AM1 over another widely used semiempirical method, modified neglect of differential overlap (MNDO), has been more widely recognized. We have carried out full geometrical optimization,²⁰ including H atoms, using a MOPAC-6.0 program, UNIX version, DEC-3100 Edition-1990. Computational details²⁰ and comparisons of PM3, AM1, and MNDO calculations and geometries are given elsewhere.

The ground-state bond lengths of tS collected in Table I represent both x-ray data²¹⁻²³ and theoretical methods.^{3,8} As expected, deviations from the idealized structure are small. Similar comparisons of bond angles show less than 3° deviations for the ring angles or for 7-1-6, within agreement with experiment except for QCFF. The 1-7-7' angle is around 126° both experimentally and theoretically. We note that MNDO and QCFF systematically overestimate bond lengths, and that PM3 is closest in this case to *ab initio* STO 3-21G results.⁸

The planarity of tS is more delicate, although recent molecular-beam results with resolved vibrational^{24,25} and rotational⁵ spectra clearly establish a planar C_{2h} ground state. The tS crystal has two inequivalent molecules per unit cell, both at inversion centers.²¹ The phenyl rings are twisted by 5° from the vinyl plane, a value that has been confirmed²³ by reanalyzing tS crystals with disordered sites. Recent calculations⁸ suggest a planar structure with a very flat potential for ring twists up to 20°–30°.

The barrier for ground-state rotation about a single bond is shown in Fig. 2 for PM3, AM1, and MNDO.

TABLE I. Experimental and theoretical C-C bond lengths, in Å, for planar *trans*-stilbene, following the labeling in Fig. 1(a).

Bond	Expt. ^a	Expt. ^b	PM3	3-21G ^c	QCFF ^d	AM1	MNDO
C1-C2	1.391	1.406	1.399	1.394	1.422	1.407	1.417
C2-C3	1.382	1.393	1.388	1.380	1.404	1.394	1.406
C3-C4	1.376	1.394	1.391	1.386	1.406	1.394	1.403
C4-C5	1.369	1.391	1.391	1.382	1.406	1.395	1.406
C5-C6	1.375	1.390	1.389	1.383	1.405	1.392	1.403
C6-C1	1.379	1.401	1.399	1.394	1.421	1.407	1.422
C7-C1	1.478	1.472	1.457	1.477	1.477	1.453	1.473
C7-C7'	1.300	1.336	1.342	1.325	1.359	1.344	1.356

^aReference 22.

^bReference 21.

^cReference 8.

^dReference 3.

Ring rotations and rotational defects in PPV are also low-energy processes^{26,27} that may have an important role in limiting the conjugation length. More accurate molecular results for tS thus have direct bearing on PPV. One ring was rotated in Fig. 2 while keeping the remaining structure planar, without any structural relaxation. The MNDO minimum at a twist $\sim 60^\circ$ does not agree with experiment. Both AM1 and PM3 indicate a planar structure, with the latter clearly stiffer, and both underestimate the barrier compared to *ab initio* calculations⁸ by $\sim 50\%$. The gas-phase quantum for rotation²⁴ about a single bond, ν_{37} , is only 8 cm^{-1} in S_0 . An anharmonic torsional potential for the ν_{37} overtones gives²⁵ a barrier height of 300 cm^{-1} , as compared to 700 cm^{-1} in Fig. 2, and the height hardly decreases in a relaxed PM3 calculation. While the rotational potential for ν_{37} remains challenging, the small barrier supports the PM3 result and rationalizes small twists in solutions, glasses, or crystals.

The planar QCFF and PM3 structures also account for the tS rotational constants of 2611.3(7.7), 262.86(2), and 240.56(2) MHz along the three principal axes of inertia.⁵ The QCFF and PM3 values deviate, respectively, by +1.8% and +3.3% for the largest component, by -0.5% and +4.0% for the next, and by -1.0% and +2.8% for the smallest, without rms corrections for deviations from planarity. Fluorescence from the excited singlet state has also been resolved and indicates a planar geometry.⁵ The rotational constants in S_1 change by -71.14(6), 5.928(4), and 3.963(4) MHz, respectively, from the ground-state values. The corresponding QCFF changes from S_0 to S_1 are -61.0, 2.8, and 1.8 MHz.

B. Excited-state geometries

In Table II we list PM3 bond lengths for the lowest singlet and triplet excited states of planar tS and for the ground state of planar ions. The bond lengths in the vinyl moiety are reversed as expected for a quinoidal structure in Fig. 1(b), which summarizes the triplet and dianion results. The bond angles are within a few degrees²⁰ of 120° for both excited states and ions. There are fewer excited-state calculations for tS, with QCFF³ and PM3 bond lengths in general agreement. The PM3 shortening

of 1-7 for the singlet is the same, while the 7-7' lengthening in Table II is 0.040 Å rather than 0.076 Å and the ring bond lengths change in the same direction but slightly less (<0.02 vs $<0.03\text{ Å}$). The changes of the PM3 rotational constants from S_0 to S_1 are -38.2, 3.03, and 2.11 MHz, respectively, comparable to the QCFF values above and within 4% of the measured rotational constants. The shortening of 1-7 in the singlet excited state raises²⁴ the ν_{37} vibrational quantum for ring rotation from 8 to 48 cm^{-1} .

The closely similar bond lengths of positive and negative ions in Table II are not required in PM3, but are understood in terms of π -electron theory¹⁶ for models with electron-hole ($e-h$) symmetry²⁸ and consequently equal bond orders for positive and negative ions. The crystal structures²⁹ of two Li salts of tS^{2-} both have disordered C7 sites. Their average 7-7' bond length of $1.42(5)\text{ Å}$ is consistent with the PM3 value of 1.440 Å in Table II. Both crystals have Li^+ ions above and below the double bond,²⁹ with planar tS^{2-} insured by a mirror plane in one

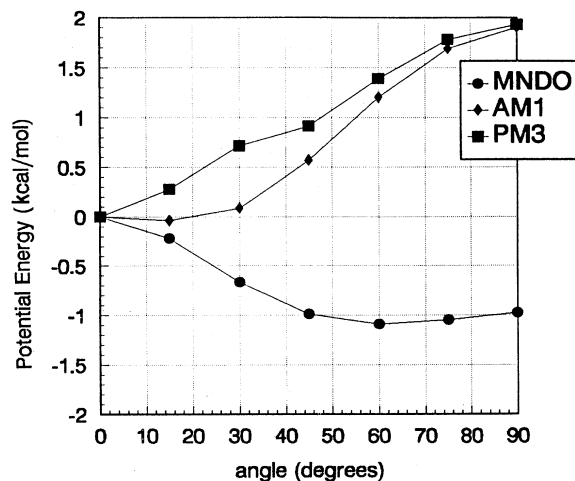


FIG. 2. PM3, AM1, and MNDO potentials for ring rotation about a single bond for ground-state tS.

TABLE II. PM3 bond lengths, in Å, of planar *trans*-stilbene in the ground (*G*) state, singlet (*S*) and triplet (*T*) excited states, and of its cation (tS⁺), anion (tS⁻), dication (tS²⁺), and dianion (tS²⁻) in the ground state; the atoms are labeled according to Fig. 1(a).

Bond	<i>G</i>	<i>S</i>	<i>T</i>	tS ⁺	tS ⁻	tS ²⁺	tS ²⁻
C1-C2	1.399	1.416	1.427	1.420	1.417	1.451	1.446
C2-C3	1.388	1.389	1.377	1.380	1.379	1.366	1.365
C3-C4	1.391	1.388	1.396	1.399	1.394	1.415	1.406
C4-C5	1.391	1.401	1.397	1.397	1.394	1.409	1.401
C5-C6	1.389	1.379	1.377	1.382	1.381	1.371	1.369
C6-C1	1.399	1.418	1.428	1.419	1.417	1.453	1.445
C7-C1	1.457	1.415	1.381	1.412	1.412	1.367	1.367
C7-C7'	1.342	1.402	1.457	1.397	1.388	1.455	1.440

case and almost planar tS²⁻ at an inversion center in the other. The average 1-7 distance of 1.48(5) Å corresponds to a single bond and clearly disagrees with the PM3 value of 1.36 Å. The phenyl bond lengths are about 0.02 Å shorter than the PM3 values, but are otherwise quite consistent with Table II.

Although PM3 focuses on accurate geometries, the energy minimization also provides excitation energies and relaxation energies relative to the ground state. The singlet (1^1B_u) and triplet (1^3B_u) excitations in Table III are 4.04 and 2.01 eV, respectively, in excellent agreement with tS spectra^{5,30} discussed in Sec. III. The electron affinity of tS is large, 1.08 eV, and its ionization potential of 8.14 eV is close to the adiabatic gas-phase value²⁵ of 7.66 eV. We calculated vertical PM3 excitation energies by relaxing all excited-state orbitals in the (frozen) ground-state geometry. The relaxation energies E_r in Table III are the differences between vertical and adiabatic PM3 excitations. Independent estimates of E_r are discussed in Sec. IV for confined singlet, triplet, and charged bipolarons.

III. EXACT PPP RESULTS AND tS SPECTRA

A. Vertical PPP excitations

The 14 π electrons of tS are typically described by a PPP model. PPP models invoke a zero-differential-overlap (ZDO) approximation¹⁴ and are usually restricted to electron transfers t between bonded sites. We note that many choices³¹ remain for the magnitude and distance dependences of $t(R)$, for the site energies ϵ (Hückel α), and for Coulomb interactions $V(R)$. PPP models have a large but finite basis and thus can be solved exactly,³² with full CI. As discussed in connection with polyenes,^{33,16} the relative position of the lowest covalent ($2^1A_g^+$) and ionic ($1^1B_u^-$) states is sensitive to correlations and doubly excited configurations³⁴ (DCI) are minimally required.

The bond lengths and bond angles of the idealized planar tS in Fig. 1(a) are standard. We retain PPP parameters for polyenes,¹⁶ with $t(R_0) = -2.40$ eV, $t_0(1 \pm \delta)$ and $\delta = 0.07$ for double and single bonds, equal site energies, and the Ohno potential³⁵ $V(R)$ with $V(0) = 11.26$ eV. Such a generic structure and parametrization amount to a parameter-free description of tS that in principle ap-

plies to any hydrocarbon. The C_{2h} point group leads to A_g and B_u electronic states, while equal site energies and nearest-neighbor t 's lead to electron-hole ($e-h$) symmetry.²⁸ We choose even (+) $e-h$ symmetry for covalent states, including the $1^1A_g^+$ ground state, and odd (-) $e-h$ symmetry for ionic states that rigorously exclude admixtures of purely covalent VB diagrams. The total spin S is also conserved.

Diagrammatic valence-bond methods¹⁸ then yield the first exact solutions, or complete CI, of the PPP model for tS. There are some 2.8×10^6 and 5.0×10^6 linearly independent singlet and triplet VB diagrams, respectively, and sparse-matrix methods are essential for extracting eigenvalues, transition moments, and other properties. The results are consequently definitive for the chosen model, completely fixing the number and position of low-lying covalent states. We may also anticipate with some confidence, based on smaller conjugated molecules,³² the effects of small changes in the parameters of site energies or of lower-symmetry structures. We have not optimized parameters, however, since guidelines are not available and each state requires 10–20 h of CPU time on a Silicon Graphics 240D computer.

The lowest two singlet and triplet excitations in each symmetry are listed in Table IV and compared with previous PPP calculations. Ting and McClure³⁶ included singly excited configurations (SCI) for slightly different parameters: $t_0 = -2.37$ eV, $V(0) = 10.59$ eV, a different $V(R)$ for small separation, and adjustable $t_s = 2.24$ eV,

TABLE III. Adiabatic PM3 excitation energies $E(X) - E_0$ (eV) for state X and relaxation energies $E_g(X) - E(X)$ relative to the ground-state geometry.

X	$E(X) - E_0$	$E_g(X) - E(X)$
1^1B_u	4.05 (3.997) ^a	0.228
3^1B_u	2.01 (2.13) ^b	0.616
tS ⁻	-1.08	0.174
tS ⁺	8.13 (7.66) ^c	0.207
tS ²⁻	1.63	0.824
tS ²⁺	20.01	0.950

^aExperiment, Ref. 5.

^bExperiment, Ref. 30.

^cExperiment, Ref. 25.

TABLE IV. Vertical PPP excitation energies, in eV, of *trans*-stilbene. Eight singlets S_n and triplets T_n , the lowest two in each subspace, are for complete CI. The SCI and selected SCI-DCI results are for slightly different parameters mentioned in the text. Oscillator strengths are given in parentheses.

State	Symmetry	PPP (full CI)	PPP (SCI-DCI) ^a	PPP (SCI) ^b
S_1	B_u^+	3.970	4.69	4.788
S_2	A_g^+	3.972	4.67	4.800
S_3	B_u^-	4.381 (0.762)	4.05 (1.11)	4.240 (0.659)
S_4	A_g^+	4.799	4.71	5.137
S_5	A_g^-	5.361	5.65	6.013
S_6	B_u^+	5.393	5.50	7.135
S_7	B_u^-	5.847 (0.420)	5.99 (0.34)	5.791 (0.406)
S_8	A_g^-	6.080	5.94	6.624
T_1	B_u^+	2.519		2.325
T_2	A_g^+	3.434		3.622
T_3	B_u^+	3.815		4.059
T_4	A_g^+	4.039		4.335
T_5	B_u^-	5.210		4.683
T_6	A_g^-	5.215 (0.011)		4.800 (0.02)
T_7	A_g^-	6.271 (0.948)		6.056 (0.93)
T_8	B_u^-	7.051		

^aReference 3.

^bReference 36.

$t_d = 2.49$ eV for the partial single and double bonds to optimize the experimental comparison. They did not use $e-h$ symmetry. Negri, Orlandi, and Zerbetto³ included 200 singly and doubly excited configurations derived from the five highest occupied and five lowest unoccupied molecular orbitals (MO's). Their $t(R)$, $V(R)$, and ϵ (which breaks $e-h$ symmetry) are taken from QCFF and contain additional parameters⁴ for fitting the ground-state and $1^1B_u^-$ potential surfaces. The relative amount of CI is nevertheless the principal reason for the different ordering of singlet and triplets in Table IV.

Electron-electron correlations lower the energies of covalent states (with positive $e-h$ index in our notation) relative to ionic state with opposite $e-h$ symmetry. At least four covalent triplets occur below the first ionic triplet in Table IV and the lowest singlets are also covalent. Less complete CI leads to an ionic S_1 , $1^1B_u^-$, whose large oscillator strength is given in Table IV. The ordering of the lowest singlets of tS is still open, as discussed below, and may be reversed in the gas and solid state. We note that the excitations in Table IV are vertical and that an ionic S_1 requires weaker Coulomb interactions in tS than in polyenes.

B. Localized and extended Hückel states in tS and PPV

In order to understand the PPP excitations, we consider localized states based on the degenerate benzene MO's and states extended over the whole molecule, instead of the exciton model of Longuet-Higgins and Murrell.³⁷ The exciton model has been used by Dyck and McClure² for the tS fluorescence and absorption, by Hohlneicher and Dick⁷ for two-photon spectra, by Orlandi, Palmieri, and Poggi,³⁸ and by others. The motivation is to rationalize the π -electronic states of tS in terms of familiar excitations of benzene and ethylene. There is strong mixing,

however, and we prefer a different decomposition into localized and extended states for interpreting the correlated PPP excitations. The natural connection is then to polyenes.

Since Hückel models reflect only connectivity, the topological symmetry of tS is D_{2h} instead of the C_{2h} structural symmetry in Fig. 1(a). Even-parity Hückel orbitals in D_{2h} have a_g or b_{1g} symmetry, while odd-parity orbitals transform as b_{2u} or b_{3u} . We take,⁹ in Fig. 1,

$$\phi_{2,3}^{(\pm)} = (\phi_{2,3} \pm \phi_{6,5}) / \sqrt{2}, \quad (1)$$

and similar combinations for the other ring. The odd linear combinations in (1) are localized on each benzene, lead to a bonding and antibonding pair at $\pm t_0$ and form b_{1g} or b_{2u} MO's for tS. The even combination in (1) leads to a_g or b_{3u} MO's that extend over the ethylene and both benzenes. The transfer integral with adjacent bridgehead carbons is $\sqrt{2}t_0$. The extended system of ten sites resembles a polyene with anomalously large alternation:⁹ in units of t_0 , the transfer integrals are $\sqrt{2}$, 1, $\sqrt{2}$, $1-\delta$, $1+\delta$, $1-\delta$, $\sqrt{2}$, 1, and $\sqrt{2}$.

In Hückel theory, the highest occupied molecular orbital (HOMO) and lowest unoccupied molecular orbital (LUMO) are extended states, while the next filled or empty MO's are degenerate localized states. The same situation⁹ holds in styrene and biphenyl, while the three rings in distyrylbenzene lead to two filled and empty extended states above and below, respectively, the filled and empty triply degenerate localized states. Low-lying excitations involving two extended states have transition dipoles close to the long axis. Long- and short-axis polarization becomes exact in D_{2h} symmetry, with 180° ethylenic bond angles for tS, and this approximate symmetry is quite useful.

Coulomb interactions $V(R)$ in the PPP model preclude

rigorous separation into localized and extended states. The unambiguous identification⁹ of correlated states is nevertheless possible by comparing the phases of selected VB diagrams with interchanged sites 2 and 6 or 3 and 5. Any excitation can consequently be identified as involving extended or localized Hückel states, even though the correlated states involve CI of more than 10^6 Hückel states. Long- and short-axis polarization of transition dipoles is regained for correlated states in D_{2h} symmetry, with 180° ethylenic bond angles.

The lowest two singlets around 3.97 eV in Table IV are covalent states involving electron transfer between localized and extended states; the degeneracy in Hückel theory is hardly lifted. The triplet pair around 5.21 eV also illustrates electron transfer between localized and delocalized states. The lowest triplets are all covalent, as expected. One-photon (dipole) selection rules connect the $1^1A_g^+$ ground state and B_u^- singlets, while two-photon selection rules are to higher A_g^+ singlets. We begin with the richer two-photon spectrum.

C. One- and two-photon spectra

Hohlneicher and Dick⁷ have recorded two-photon spectra of tS at 77 K in 3-methylpentane. Two weak bands *a* and *b* around 3.9 and 4.4 eV are followed by a strong band *c* around 5.0 eV and a very weak feature *d* around 5.7 eV. We agree with Orlandi, Palmieri, and Poggi³⁸ in assigning band *c* to the $3^1A_g^+$ transition at 4.80 eV in Table IV. The broad band *c* extends from ~ 4.7 to 5.2 eV and shows vibronic structure. Since $3^1A_g^+$ is an extended state, both transition moments connecting it to the ground state are roughly along the long axis. The two-photon intensity for circularly polarized light³⁹ is then $\sim \frac{2}{3}$ of the intensity for linearly polarized light, as observed in band *c*.

We have not carried out DVB calculations⁴⁰ for the complete two-photon intensities⁴¹ for $2^1A_g^+$ at 3.97 eV and $3^1A_g^+$. The contributions from virtual states $1^1B_u^-$ and $2^1B_u^-$ suggest 20 times less two-photon intensity for $2^1A_g^+$. The combined intensities of bands *a* and *b* are at least an order of magnitude less than *c*'s. Moreover, $2^1A_g^+$ involves a localized-extended transition and, for D_{2h} symmetry (180° ethylene bond angles), transforms as B_g^+ ; the transition dipoles for two-photon absorption are then required to be orthogonal and the intensity ratio for circular and linear polarization⁴⁰ becomes 1.5. The observed⁷ ratio is ~ 1 in the *a*-*b* region. The near degeneracy of $2^1A_g^+$ and $1^1B_u^+$ implies that small perturbations of 0.1 eV strongly admix these states, provided that inversion symmetry is lifted for a nonplanar structure. In the glass, we consequently propose that bands *a* and *b* are linear combinations of $2^1A_g^+$ and $1^1B_u^+$, with similar two-photon intensities due to $2^1A_g^+$. The very weak feature (*d*) may then be associated with A_g^+ admixture in $2^1B_u^+$ at 5.39 eV in Table IV.

The intense one-photon absorption to $1^1B_u^-$ is around 3.70 eV in 3-methylpentane,⁷ at 3.997 eV in the gas phase,⁵ and has been extensively studied both in absorption and emission.^{2,42,43} While both the ground and excited states have rich vibrational spectra, as has already

been noted, we are interested here in the position and intensity of the $1^1B_u^-$ absorption. The 0-0 line has been resolved for tS in molecular beams⁵ (3.996 51 eV) and in dibenzyl crystals² (3.7074 eV). The difference of 0.3 eV is the larger solid-state shift expected for the more polarizable,⁴⁴ ionic excited state. The adiabatic excitation is less than the vertical excitation at 4.38 eV in Table IV. Solid-state spectra place 0-0 for $1^1B_u^-$ below any even-parity state.

The situation in the gas phase is relevant for testing PPP models and, even after estimating relaxation energies in the next section, leads to the ordering in Table IV. Standard PPP parameters also overestimate $1^1B_u^-$ slightly in polyenes¹⁶ or in naphthalene.⁴⁵ The exact PPP transition dipole is 6.77 D, which gives an oscillator strength of $f=0.76$ for $1^1B_u^-$. The resulting radiative lifetime is within 10% of the 2.7 ± 0.1 ns measured⁴² in supersonic jets. The second one-photon absorption, to $2^1B_u^-$, is⁷ around 5.3 eV in 3-methylpentane at 77 K, around⁴⁶ 5.5 eV in ethanol at 300 K, and at 5.84 eV in Table IV. Its oscillator strength is 0.420, slightly over half the $1^1B_u^-$ value. The observed intensities are even more disparate,^{46,7} with the second band slightly less than half as intense as the first.

D. Triplet and dianion states

The 0-0 transition of the tS triplet is at 2.13 eV, as found precisely in emission³¹ and approximately in absorption,² while the vertical PPP excitation in Table IV is 2.52 eV. The relaxation energy for the triplet bipolaron is substantial, as suggested by the structural changes in Table II. The fine-structure constants and principal axes provide⁴⁵ a sensitive test of the $1^3B_u^+$ wave function. The observed values⁴⁷ are $D=0.101$ and $E=0.025$ cm^{-1} , with the principal axis in the molecular plane 12° from the central double bond. We obtain $D=0.127$, $E=0.027$ cm^{-1} , and the principal axis 7° from the double bond. As in other organic triplets, dipole-dipole interactions between the two unpaired electrons dominate and there are no free parameters. To illustrate the strong r^{-3} dependences of *D* and *E*, we also used the PPP spin correlations of $1^3B_u^+$ for the PM3 triplet geometry in Table II. We find $D=0.119$, $E=0.026$ cm^{-1} , and the principal axis 10° from the double bond. The agreement is excellent, especially for an idealized structure and standard hydrocarbon parameters.

Dipole transitions from $1^3B_u^+$ to $1^3A_g^-$ and $2^3A_g^-$ are calculated to be at 2.70 and 3.75 eV, respectively, with transition dipoles of 1.02 and 8.16 D. The oscillator strength of the second transition is almost 90 times higher, as shown in Table IV, in agreement with PPP-SCI calculations. The triplet-triplet excitation at 3.28 eV reported by Herkstroeter and McClure⁴⁸ is assigned to $2^3A_g^-$, both on account of its estimated oscillator strength of 0.51 and our overestimation of one-photon excitations. Within the PPP model, these is a clear prediction of another weak triplet-triplet excitation around 2.3–2.5 eV.

We have also carried out exact PPP calculations for tS^{2-} or tS^{2+} , whose spectra coincide exactly in models

with $e-h$ symmetry. We again used the planar geometry in Fig. 1 and standard PPP parameters. The bipolaron ground state is 1^1A_g , with excitation energies of 0.7285 eV to 2^1A_g , 0.7346 eV to 1^1B_u , and 2.2321 eV to 2^1B_u . The calculated transition dipoles are 0.694 D to 1^1B_u and 9.446 D to 2^1B_u . The more intense transition coincides nicely with the 2.5 eV band of tS^{2-} in solution.⁴⁹ The ir excitation has not been reported, to the best of our knowledge, and involves another pair of nearly degenerate states related to electron transfer between localized and extended states.

Exact PPP results for tS provide a comprehensive and consistent picture of its low-lying states, without, however, offering detailed vibrational analyses of S_0 , S_1 , or T_1 . Higher-energy states can be added to Table IV and different parameters or geometries can readily be probed. Relaxing $e-h$ or inversion symmetry essentially doubles the PPP matrices. Weak one-photon transitions to B_u^+ states occur when $e-h$ symmetry is broken,⁴⁵ with weaker oscillator strengths $\sim 10^{-3}$ – 10^{-4} compared to $1^1B_u^-$. Such “forbidden” transitions occur in styrene, biphenyl, or naphthalene below the lowest intense absorption.⁹ Detection of weak $1^1B_u^+$ absorption could be much more difficult above the 0-0 line of $1^1B_u^-$. We have found it advantageous to retain $e-h$ and C_{2h} symmetry and then examine the consequences of symmetry breaking. The PPP matrices of the radical ions tS^+ and tS^- in C_{2h} are also about twice that of singlet tS , and thus just beyond DVB solution with a Silicon Graphics 240D. The spectra of tS^+ and tS^- are identical in PPP models with $e-h$ symmetry. Full CI for ion-radical and broken-symmetry tS states will shortly be accessible.

IV. RELAXATION ENERGIES AND tS BIPOLARONS

A. PPP bond orders and PM3 bond lengths

The PPP excitations in Table IV are vertical transitions for the idealized geometry in Fig. 1(a). The adiabatic PM3 excitation energies in Table III, on the other hand, involve differences between relaxed SCF solutions for planar species. The relaxation energy E_r is sketched in Fig. 3 for a single nuclear coordinate. Except for zero-point differences between the normal modes in the ground and excited states, resolved 0-0 lines are adiabatic excitations and the maxima of unresolved spectra are approximately vertical excitations. In view of the ~ 0.3 -eV uncertainties of PPP excitation energies, however, the distinction between vertical and adiabatic excitations is rarely essential.

Much larger E_r may be associated with charged species, and comparisons among $E_r(X)$ for different excited states X require more accurate determination. The relaxation energy is also the polaron or bipolaron binding energy that, in solid-state models of conjugated polymers,¹³ is due to linear e -ph coupling. Spectroscopic signatures¹² of self-localized polymeric states have been widely recognized in polyacetylene, polythiophenes, and other conjugated polymers. Their assumed applicability to PPV has recently been questioned,¹⁷ however, due to its small Stokes shift of 100 cm^{-1} or less for the singlet

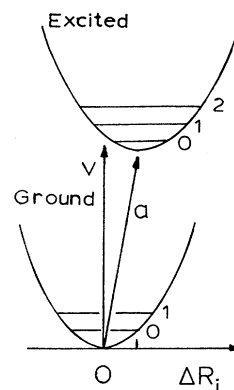


FIG. 3. Schematic ground- and excited-state potentials for vertical and adiabatic excitations.

bipolaron. Confined bipolarons of tS give upper bounds for $E_r(X)$ in harmonic systems with linear e -ph coupling.

Several issues must be addressed for accurate evaluations of $E_r(X)$. An *ab initio* or semiempirical calculation dispenses with assumptions about σ -electron contributions, but is limited in practice to modest CI. The opposite approach is taken in π -electron theory, with full CI now possible for tS . But the geometry must largely be assumed and geometry optimization calls for PM3 or related methods. Since the PM3 excited states in Table III clearly involve the π MO's, we start by comparing their geometries in Table II with PPP results.

The π -electron bond order introduced by Coulson⁵⁰ can readily be defined for the PPP model,

$$p_i = (\partial E_0 / \partial t_i) / 2 = - \sum_{\sigma} \langle G | a_{i\sigma}^{\dagger} a_{j\sigma} + a_{j\sigma}^{\dagger} a_{i\sigma} | G \rangle / 2. \quad (2)$$

Here sites i and j are bonded, $a_{i\sigma}^{\dagger}$ ($a_{i\sigma}$) creates (annihilates) a π electron at site i , and the expectation value is over the ground state. The expectation value with respect to $|X\rangle$ gives excited-state bond orders. Exact PPP bond orders for the tS ground and bipolaronic states are compared in Table V with PM3 bond lengths. The detailed agreement between increasing R and decreasing $p(R)$, even for the small variations of the phenyl bond lengths, is shown in Fig. 4. Except for two miniscule ΔR of 0.001 and 0.003 Å, ΔR and Δp have opposite signs for the singlet, triplet, and charged tS bipolaron. Empirical correlations between bond orders and bond lengths have indeed been proposed,¹⁵

$$R = a - bp(R). \quad (3)$$

Hückel bond orders for sp^2 - sp^2 carbons lead⁵¹ to $a \sim 1.5$ Å and $b = 0.15, 0.18, \text{ or } 0.20$ Å. PPP bond orders lead in Fig. 4 to $b = 0.25$ Å, as shown by the dashed line, and only the slope is needed for relaxation energies. We will use the PM3 geometries whenever possible and the linear relation (3) with $b = 0.25$ Å in other cases.

B. Approximation for E_r

The central problem is to combine accurate molecular geometries with as complete CI as possible. The bond

TABLE V. Stilbene bond lengths (\AA) and π -bond orders [Eq. (2)], labeled according to Fig. 1(a); excited state values are relative to the $1^1A_g^+$ ground state.

State	Ring bonds						Bridge bonds	
	12	16	23	56	34	45	17	77'
$1^1A_g^+$, R (\AA)	1.399	1.399	1.389	1.388	1.391	1.391	1.457	1.342
p	0.607	0.610	0.655	0.646	0.636	0.639	0.309	0.855
$1^1B_u^-$, ΔR (\AA)	0.019	0.017	-0.010	0.001	0.010	-0.003	-0.042	0.060
Δp	-0.129	-0.142	0.044	0.034	-0.059	-0.036	0.197	-0.397
$1^3B_u^+$, ΔR (\AA)	0.029	0.028	-0.032	-0.011	0.006	0.005	-0.076	0.115
Δp	-0.116	-0.118	0.022	0.031	-0.045	-0.048	0.227	-0.495
tS^{2+} , ΔR (\AA) ^a	0.054	0.052	-0.018	-0.022	0.015	0.024	-0.090	0.113
ΔR (\AA)	0.046	0.047	-0.020	-0.023	0.010	0.018	-0.090	0.098
Δp	-0.184	-0.175	0.073	0.094	-0.096	-0.129	0.285	-0.302
$2^1A_g^+$, Δp	-0.096	-0.098	-0.102	-0.092	-0.068	-0.073	0.086	-0.088
$1^1B_u^+$, Δp	-0.095	-0.099	-0.102	-0.093	-0.069	-0.073	0.086	-0.087
$3^1A_g^+$, Δp	-0.230	-0.234	0.071	0.081	-0.134	-0.136	0.317	-0.528
$1^3A_g^-$, Δp	-0.073	-0.079	-0.087	-0.078	-0.048	-0.052	0.083	-0.082
$2^3A_g^-$, Δp	-0.167	-0.166	0.057	0.065	-0.095	-0.102	0.158	-0.309

^aBipolaron; PM3 bond lengths for ± 2 ; PPP bond orders are equal by e - h symmetry.

lengths R_i appear in $t(R_i)$ and give the most important structural dependences in π -electron theories. In PPP models with equal site energies, for example, the electronic energy in state $|X\rangle$ is

$$E(X) = \sum_i 2t(R_i)p_i + \sum_r V(0)\langle X|q_r(q_r-1)|X\rangle/2 + \sum_{r>s} V(R_{rs})\langle X|q_rq_s|X\rangle. \quad (4)$$

The first sum is over all bonds, involves the bond order (2) for $|X\rangle$, and is the only contribution in Hückel theory. The second sum is over all sites, involves the π -electron charge operator $q_r = 1 - n_r$, and gives the contribution for two π electrons in the same $2p_z$ orbital. The last sum in (4) corresponds to Coulomb interactions between sites r and s and involves the charge-correlation functions $\langle q_rq_s \rangle$. The Ohno potential³⁵ $V(R)$ interpolates between $V(0) = 11.26$ eV for carbon and e^2/R at large separation,

$$V(R) = e^2/(\rho^2 + R^2)^{1/2}, \quad (5)$$

where $\rho = V(0)/e^2 = 1.28$ \AA is the effective separation between two π electrons in the same $2p_z$ orbital. A linear or exponential choice for $t(R)$ then completely fixes the variations of $E(X)$ with molecular geometry. We note that (4) also provides the first-order correction for parameter changes, when neither the bond orders nor charge-correlation functions change.

At the π -electron level, the total energy E_T has additive π and σ contributions, and the latter are independent by hypothesis of the π -electronic state $|X\rangle$. The equilibrium condition with respect to any geometrical change leads for bond lengths to

$$(\partial E_T / \partial R_i)_0 = (\partial E_0 / \partial R_i)_0 + (\partial E_\sigma / \partial R_i)_0 = 0, \quad (6)$$

where E_0 is the π -electron ground state and the partials are evaluated at equilibrium. We use (6) to obtain the variation of the total energy in excited state $|X\rangle$ with

each R_i ,

$$(\partial E_{TX} / \partial R_i)_0 = (\partial E_X / \partial R_i)_0 - (\partial E_0 / \partial R_i)_0. \quad (7)$$

The slope of the potential at ΔR_i from the excited-state equilibrium leads, as sketched in Fig. 3, to

$$E_r(X) = - \sum_i (\partial E_{TX} / \partial R_i)_0 \Delta R_i / 2 \quad (8)$$

for the relaxation energy in the harmonic approximation for C-C stretches ΔR_i . Since (8) is linear in ΔR_i and $\partial/\partial R_i$, we can replace R_i with normal coordinates Q_i , in the same approximation. As discussed by Salem,¹⁵ the Taylor expansion should be carried out to second order. The estimate (8) is consistent with the PM3 values for E_r

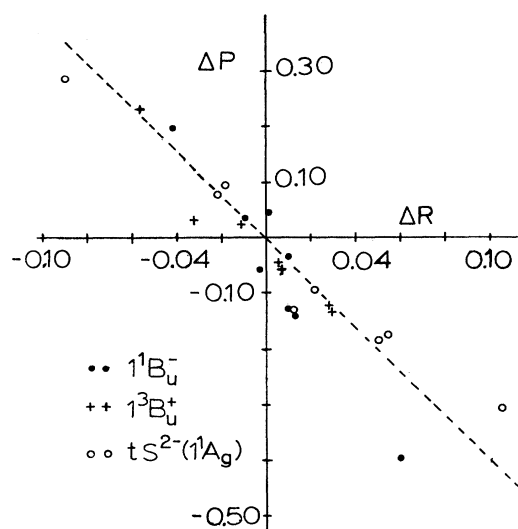


FIG. 4. PPP bond orders vs PM3 bond lengths for singlet, triplet, and charged tS bipolarons; the dashed line has slope 0.25 for the linear relation in Eq. (3).

TABLE VI. PPP charge-correlation functions $\langle q_i q_j \rangle$ for bonded sites in Fig. 1(a); excited-state values $\Delta\langle q_i q_j \rangle$ are relative to the $1^1A_g^+$ ground state of *trans*-stilbene.

State	Ring bonds						Bridge bonds	
	12	16	23	56	34	45	17	77'
$1^1A_g^+$	-0.1856	-0.1881	-0.2069	-0.2052	-0.2011	-0.2023	-0.0704	-0.2894
$2^1A_g^+$	0.0350	0.0357	0.0331	0.0315	0.0220	0.0239	-0.0242	0.0440
$3^1A_g^+$	0.0877	0.0902	-0.0201	-0.0221	0.0585	0.0598	-0.1353	0.1845
$1^3B_u^+$	0.0499	0.0526	-0.0049	-0.0064	0.0217	0.0230	-0.0599	0.1993
$1^1B_u^-$	-0.0062	-0.0161	-0.0400	-0.0375	-0.0041	-0.0109	-0.1745	-0.0541
$2^1B_u^-$	-0.0308	-0.0298	-0.0785	-0.0352	-0.0805	-0.0747	-0.0179	-0.0335
$1^1A, tS^{2+}$	0.0822	0.0781	-0.0215	-0.0303	0.0567	0.0717	-0.0798	0.1682

in Table III, which do not involve a Taylor expansion. We further approximate E_r by using (3) to estimate ΔR_i when the excited-state geometry is not available.

The partial derivatives in (8) are readily found from the PPP energies (4)

$$(\partial E_{TX}/\partial R_i)_0 = 2t'(R_i)\Delta p_i + V'(R_i)\Delta\langle q_i q_j \rangle, \quad (9)$$

where Δp_i is the bond-order change between $|X\rangle$ and $|G\rangle$, and $\Delta\langle q_i q_j \rangle$ is the corresponding change in the charge-correlation function of bonded sites. The generic PPP parameters lead to $t' = t_0\delta/\Delta R = 3.36$ eV/Å, since $\Delta R = \pm 0.05$ Å for single and double bonds gave transfer integrals $t_0(1 \pm \delta)$, respectively, with $t_0 = -2.40$ eV and $\delta = 0.07$. Molecular choices for t' are in this range, while solid-state values⁵² of 8 eV/Å are needed to model polyacetylene with noninteracting π electrons. The Ohno potential (5) leads to $V' = -2.95$ eV at 1.40 Å.

The relaxation energy (8) is then obtained by using (9),

$$E_r(X) = - \sum_i [2t'\Delta p_i + V'\Delta\langle q_i q_j \rangle] \Delta R_i / 2. \quad (10)$$

The sum is over all bonds and t' and V' are constants. The first term in (8) is simply the product of the bond-order, bond-length changes in Table V. Their opposite signs and positive t' show that the energy is lowered. The nearest-neighbor charge-correlation functions in Table VI are negative, as expected for adjacent charge fluctuations of opposite sign. We list in Table VI the ground-state $\langle q_i q_j \rangle$ and $\Delta\langle q_i q_j \rangle$ changes for selected excited states. The signs of $V'\Delta\langle q_i q_j \rangle$ and ΔR_i are again almost always opposite and $E_r(X)$ increases, but the second term is 5–10 times smaller than the first.

C. Charge and spin dependence of E_r

We now have three estimates for the relaxation energy. The values in Table III are entirely based on PM3 and involve ground states. We may combine PPP energies and PM3 geometries in (10) whenever both are available, as shown in Table VII for $E_r(X)$ and the bond-order contribution. We may also use (3) to estimate bond-length changes from bond-order changes, thereby generating all the input for (10) from π -electron theory. Such entries in Table VII are in parentheses.

All three estimates give a relaxation energy of 0.2–0.3 eV for $1^1B_u^-$, the singlet bipolaron, and 0.4–0.6 eV for $1^3B_u^+$, the triplet bipolaron. E_r is largest for charged bi-

polarons, ~ 0.5 eV in Table VII and ~ 0.9 eV in Table III. In solid-state models based on Hückel theory, any alternant hydrocarbon like tS has closely related HOMO and LUMO that are equally bonding and antibonding, respectively. An excitation across the gap, whether leading to a singlet or triplet state, then gives the same E_r . Moreover, the same E_r is also expected on adding or removing two electrons. The bipolaron binding energies of tS clearly depend on both spin and charge, with the smallest E_r for $1^1B_u^-$ and the largest for tS^{2+} or tS^{2-} . The larger e -ph coupling constant $\alpha = (dt/dR)_0 \sim 8$ eV in solid-state models can be adjusted to fit charged polarons, but misses the dependence on charge and spin and disagrees with molecular data.

The near degeneracy of $1^1B_u^+$ and $2^1A_g^+$ also extends to their bond orders in Table V. Their small E_r is ~ 0.10 eV in Table VII. The vertical gap of 0.39 eV between the lowest excited covalent and ionic singlets in Table IV is cut in half on including E_r 's. Such small splittings may be beyond the limits of standard PPP parameters and possibly even of π -electron models. The larger E_r for $1^3B_u^+$ brings the adiabatic singlet-triplet splitting down to the observed 2.1-eV region. In addition, the bond orders of $1^3B_u^+$ in Table V closely resemble those of $2^3A_g^-$, while those of $1^3A_g^-$ are closer to the ground state's. Thus E_r for a T - T transition to $2^3A_g^-$ is very small, ~ 0.05 eV, and there is reduced vibronic activity,⁴⁸ as has also been noted⁵³ for T - T spectra of PPV. We also note the large E_r of $3^1A_g^+$ in Table VII, which may require more accurate treatment. Its large Δp_i are associated with bond-order reversals found in the $2^1A_g^+$ state of polyenes, thereby providing additional evidence for identifying the $3^1A_g^+$ state of tS with extended states.

TABLE VII. Relaxation energies, in eV, of tS states based on Eq. (10); the bond-order contributions are listed separately and values in parentheses are based on $\Delta p = -4\Delta R$ in Eq. (3) and Fig. 4.

State	$E_r(X)$	$t'\Delta p$
$1^1B_u^-$	0.191 (0.290)	0.174 (0.273)
$1^3B_u^+$	0.420 (0.405)	0.362 (0.348)
$1^1A_g, tS^{2\pm}$	0.530 (0.459)	0.449 (0.389)
$2^1A_g^+, 1^1B_u^+$	(0.104)	(0.099)
$3^1A_g^+$	(0.777)	(0.665)

V. DISCUSSION

A. PM3/PPP comparisons

The PM3 and PPP results for tS bipolarons are remarkably similar. The single-determinantal PM3 excitation energies in Table III involve π electrons, although the σ MO's are reoptimized in the SCF calculation even in the case of vertical excitations. Such reorganization of the ground-state orbitals could also be represented as CI. The ground states of tS, tS^{2-} , and tS^{2+} have closed electronic shells, the best case for a single-determinantal approximation. The ground state of tS^- or tS^+ is also represented naturally by a single determinant, with a singly filled orbital, while the triplet is a single determinant with two parallel spins. Even the 1^1B_u state is the lowest odd-parity state and can be reasonably represented by a single configuration. The tS bipolarons are among the most likely to be represented well at the SCF level, while complete CI for the PPP model should also be appropriate for other π -electronic excitations.

The $e-h$ symmetry¹⁶ of tS with standard PPP parameters leads to precisely one π electron per site, in any eigenstate $|X\rangle$. The PM3 results for $|G\rangle$, $|1^1B_u\rangle$, and $|1^3B_u\rangle$ also give essentially one π electron per site. The PPP charge distributions for the 1^1A_g ground state of tS^{2-} are compared in Fig. 5 with the PM3 charges obtained from Mulliken populations. The tS^{2+} charges are exactly the opposite in PPP theory, due to $e-h$ symmetry, and are almost opposite in PM3. As noted in connection with Fig. 1(b), charged bipolarons have a more quinoidal structure and elementary VB considerations account for the principal features of the charge distribution in Fig. 5. The reduced value of q_6 in PPP theory lowers the repulsion with $q_7 = -0.18$.

The PPP and PM3 spin densities in the triplet ground state are also compared in Fig. 5. Small negative spin densities^{54,55} are quite typical for correlated states and may be understood in terms of short-range antiferromagnetic ordering. Since spin densities in MO theory are simply given by the orbital amplitudes, all the PM3 values are positive. There is again reasonable agreement. The fine-structure constants D and E provide a more

severe test, however, as discussed for the naphthalene triplet.⁴⁵ The large spin densities in Fig. 5 at the central double bond explain the sensitivity of D and E to the change between the idealized and PM3 structure, as mentioned in Sec. III.

In addition to excitation energies, PPP and PM3 calculations can also be compared for disproportionation reactions such as $2tS \rightarrow tS^{2-} + tS^{2+}$. The vertical PM3 results in Table III give 23.41 eV; the corresponding PPP result is 25.11 eV. The effective U_e for the repulsion of the two charges of a bipolaron is given by

$$2tS^\pm \rightarrow tS + tS^{2\pm} \quad (11)$$

Table III leads to $U_e = 3.74$ and 3.94 eV, respectively, for relaxed positive and negative species, which is quite reasonable for an average separation of $\sim 5 \text{ \AA}$ in tS. PPP results for polarons will allow additional comparisons. The PM3 bipolaron results plus the singlet and triplet excitation and relaxation energies are clearly in good agreement with exact PPP results. PM3/PPP comparisons thus provide some support for the widespread application of SCF methods to polarons and bipolarons in conjugated polymers.

B. Bipolaron binding energies

The different relaxation energies in Table VII for the singlet, triplet, and charged bipolarons are not surprising from a molecular point of view, although the structural similarities in Table II between the tS singlet and polarons, and between the triplet and bipolarons, are worth noting. Linear e -ph coupling in the SSH model¹¹ of conjugated polymers unequivocally leads to the same E_r for all three types of bipolarons. Indeed, this follows from the equal bonding and antibonding character of the HOMO and LUMO, whether or not e -ph coupling is taken to be linear, in Hückel or SCF solutions to π -electron models with $e-h$ symmetry. Correlation effects are partially included in noninteracting models by renormalizing¹³ t and $\alpha = dt/dR$, and such freely adjustable parameters may then rationalize differences with conjugated molecules. The different relaxation energies of confined tS bipolarons illustrate intrinsic limitations of noninteracting models.

Linear e -ph coupling, a harmonic lattice, and a constant band gap lead to decreasing E_r with increasing delocalization, since spreading the same distortion over more sites N leads to a N^{-1} dependence for E_r . Preliminary PM3 results⁵⁶ for longer oligomers indicate constant E_r for the singlet. The decreasing band gap increases the susceptibility for distortions and no linear approximation has been used. The small PPV Stokes shifts¹⁷ imply small E_r for the singlet, as found, but additional Franck-Condon analyses will be needed to test whether an E_r of ~ 0.2 eV is consistent with predominantly 0-0 fluorescence in the long-wavelength region. The larger E_r of charged tS bipolarons, on the other hand, appear to be consistent with bipolaronic interpretations of photoinduced PPV spectra.¹⁰ The tS results indicate the compatibility of small Stokes shifts and large bipolaron binding.

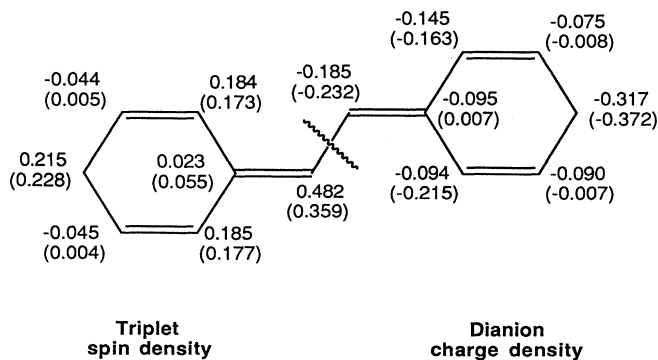


FIG. 5. Exact PPP spin densities for $1^3B_u^+$ and charge densities for the tS^{2-} ground state. PM3 results are in parentheses.

We also find e - e correlation to alter bipolaron spectra. The one-photon absorptions of $tS^{2\pm}$ at 0.73 and 2.23 eV are followed by several others below the one-photon tS gap at $E_g = 4.31$ eV in Table IV, while the SSH model leads¹² to only two bipolaronic excitations whose sum is E_g . Additional bipolaronic excitations below E_g can be rationalized in the opposite limit of strong correlations, with $V(0) \gg t$, in terms of different charge distributions in Fig. 5. But tS or polyene spectra require at most intermediate e - e correlations. The low resolution of subgap excitations in conjugated polymers precludes definitive assignments to two or more electronic states or precise comparisons to E_g .

C. One- and two-photon thresholds in tS and PPV

The close proximity of the covalent $1^1B_u^+$ and $2^1A_g^+$ states to the ionic $1^1B_u^-$ state is consistent with experiment, as shown by tS spectra in 3-methylpentane. The occurrence of another, unspecified electronic level about 0.1 eV above $1^1B_u^-$ has also been recognized in high-resolution beam data.^{42,43} Exact PPP results with standard parameters place the covalent states below $1^1B_u^-$ even when E_r is included, although splittings of ~ 0.2 eV may be beyond π -electron models. As expected for more polarizable ionic states,⁴⁴ and as shown by the 0.3-eV shift of the 0-0 tS line in dibenzyl crystals, a lowest $1^1B_u^-$ singlet in condensed phases can readily be rationalized. The puzzle with $1^1B_u^-$ also being the lowest singlet in the gas phase is primarily with the experimental requirement of almost exactly equal solid-state shifts.

Complete CI clearly leads in Table IV to a substantial splitting between $3^1A_g^+$ and the lowest covalent states, a splitting that is not apparent for partial DCI. Additional information about two-photon intensities facilitates assigning the two-photon spectrum. The greater alternation of stilbene relative to polyenes due to the transformation (1) thus places⁹ the lowest even-parity state of the extended π system well above $1^1B_u^-$. In the PPV limit, all low-lying excited states are associated with the extended states,⁹ while the highly degenerate states derived from the degenerate benzene orbitals lead to flat bands at higher energy.⁵⁷ As noted in connection with PPV fluorescence, the increased alternation due to *para*-conjugated phenyls reverses the polyene ordering of the lowest one- and two-photon states.

Coulomb interaction between the electron and hole lead to an exciton in PPP theory, a feature missed in Hubbard models restricted to on-site interactions. In conjugate polyenes with alternating transfer integrals $t(1 \pm \delta)$, there is a crossover⁵⁸ of $2^1A_g^+$ and $1^1B_u^-$ with increasing δ in PPP models with otherwise fixed parameters. The greater alternation of polysilanes, which fluoresce⁵⁹ even more strongly than PPV, is accompanied by parameter changes for the σ -conjugated silicon back-

bone.⁵⁸ Since hydrocarbon parameters for sp^2 sites are common to tS , PPV, and polyenes, they provide stronger confirmation for the role of alternation in the ordering of one- and two-photon excitations.

The increasing Hückel gap $4t\delta$ between the valence and conduction bands suggests less sensitivity to *fixed* e - e correlations with increasing δ . The charge-correlation function $\langle X|q_r^2|X \rangle$ measures the ionicity of site r in state $|X \rangle$. In models with e - h symmetry, we have⁴¹ $\langle G|q_r^2|G \rangle = 0.50$ for any half-filled Hückel band or SCF approximation to any PPP model. In the limit of strong correlation, the ionicity vanishes at every site of half-filled systems, with one electron per site. PPP parameters for finite polyenes⁴¹ lead to $\langle G|q_r^2|G \rangle \sim 0.37$. The tS values are slightly over 0.40 in the ring, 0.42 at C1, and 0.37 at 7 or 7', consistent with larger effective alternation. As in polyenes, $1^1B_u^-$ in tS is more ionic than the ground state $3^1A_g^+$ is less ionic. The ionicity and one- and two-photon excitations illustrate the interplay between alternation and intermediate e - e correlations.

D. Summary

In summary, generic parameters and exact PPP solutions account for diverse π -electronic excitations of tS , including intensity and magnetic data. The ground-state PM3 geometry and small rotational barrier about single bonds agree with resolved tS spectra. PM3 geometries for confined singlet, triplet, and charged bipolarons correlate well with π -electron bond orders. The bipolaron relaxation energies depend on both spin and charge, increasing from singlet to triplet to charged bipolarons, for both PPP and PM3 calculations. The tS and tS^{2-} excitations were related to Hückel states localized on each phenyl and extended over an alternating chain by means of a transformation that also holds for PPV. The large topological alternation due to *para*-conjugated phenyls interchanges the one- and two-photon excitations of the extended system relative to polyenes and rationalizes the different photophysics of PPV and polysilanes compared to polyacetylene and polydiacetylenes. We have emphasized the advantages of combining correlated π -electronic excitations with semiempirical structural calculations, and of relating accurate molecular data to the electronic excitation of conjugated polymers.

ACKNOWLEDGMENTS

We thank Dan Nordlund for system assistance and gratefully acknowledge support for work at Princeton University by the National Science Foundation through Grant No. NSF-DMR-8921072; Z.G.S. thanks Professor D.S. McClure for stimulating discussions; D.S.G. thanks Dr. R. Denton for fruitful discussions and the Brazilian Agency FAPESP for financial support.

¹R. J. Sension, S. T. Repinec, and R. M. Hochstrasser, *J. Chem. Phys.* **93**, 9185 (1990).

²R. H. Dyck and D. S. McClure, *J. Chem. Phys.* **36**, 2326, (1962).

³F. Negri, G. Orlandi, and F. Zerbetto, *J. Chem. Phys.* **93**, 5124 (1989).

⁴A. Warshel and M. Karplus, *J. Am. Chem. Soc.* **94**, 5612 (1972).

- ⁵B. B. Champagne, J. F. Pfanstiel, D. F. Plusquellic, D. W. Pratt, W. M. van Herpen, and M. L. Meerts, *J. Chem. Phys.* **94**, 6 (1990).
- ⁶J. J. P. Stewart, *J. Comput. Chem.* **10**, 209 (1989); **10**, 221 (1989).
- ⁷G. Hohlneicher and B. Dick, *J. Photochem.* **27**, 215 (1984).
- ⁸O. Lhost and J. L. Brédas, *J. Chem. Phys.* **96**, 5279 (1992).
- ⁹Z. G. Soos, S. Etemad, D. S. Galvão, and S. Ramasesha, *Chem. Phys. Lett.* **194**, 341 (1992); Z. G. Soos, S. Ramasesha, D. S. Galvão, R. G. Kepler, and S. Etemad, *Synth. Met.* (to be published).
- ¹⁰N. L. Colaneri, D. D. C. Bradley, R. H. Friend, P. L. Burns, A. B. Holmes, and C. W. Spangler, *Phys. Rev. B* **42**, 11 670 (1990); J. H. Burroughes, D. D. C. Bradley, A. R. Brown, R. N. Marks, K. MacKay, R. H. Friend, P. L. Burns, and A. B. Holmes, *Nature* **347**, 539 (1990); L. A. Swanson, P. A. Lane, J. Shinar, and F. Wudl, *Phys. Rev. B* **44**, 10617 (1991).
- ¹¹W. P. Su, J. R. Schrieffer, and A. J. Heeger, *Phys. Rev. Lett.* **44**, 1698 (1979); *Phys. Rev. B* **22**, 2209 (1980).
- ¹²*Handbook of Conducting Polymers*, edited by T. A. Skotheim (Marcel Dekker, New York, 1986), Vols. 1 and 2.
- ¹³A. J. Heeger, S. Kivelson, J. R. Schrieffer, and W. P. Su, *Rev. Mod. Phys.* **60**, 781 (1988).
- ¹⁴R. Pariser and R. G. Parr, *J. Chem. Phys.* **21**, 767 (1953); J. A. Pople, *Trans. Faraday Soc.* **42**, 1375 (1953).
- ¹⁵L. Salem, *The Molecular Orbital Theory of Conjugated Systems* (Benjamin, New York, 1966), Chaps. 2, 3, and 7.
- ¹⁶Z. G. Soos and G. W. Hayden, in *Electroresponsive Molecular and Polymeric Systems*, edited by T. A. Skotheim (Marcel Dekker, New York, 1988), Vol. 1, p. 197.
- ¹⁷U. Rauscher, H. Bassler, D. D. C. Bradley, and M. Hennecke, *Phys. Rev. B* **42**, 9830 (1990); D. D. C. Bradley, A. R. Brown, P. L. Burn, J. H. Burroughes, R. H. Friend, A. B. Holmes, K. D. MacKay, and R. N. Marks, *Synth. Met.* **41**, 3135 (1991).
- ¹⁸Z. G. Soos and S. Ramasesha, in *Valence Bond Theory and Chemical Structure*, edited by D. J. Klein and N. Trinajstić (Elsevier, Amsterdam, 1990), p. 81; S. Ramasesha, Bhabadyuti Sinha, and I. D. L. Albert, *Phys. Rev. B* **42**, 9098 (1990).
- ¹⁹M. J. S. Dewar, E. F. Healy, A. J. Holder, and Y. C. Yuan, *J. Comput. Chem.* **11**, 541 (1990); J. P. Stewart, *ibid.* **11**, 543 (1990); P. S. Scano and C. Thomson, *ibid.* **12**, 172 (1991).
- ²⁰D. S. Galvão, Z. G. Soos, S. Ramasesha, and S. Etemad, *J. Chem. Phys.* (to be published).
- ²¹A. Hoekstra, P. Meerteens, and A. Vos, *Acta Crystallogr. Sect. B* **31**, 2813 (1975).
- ²²J. Bernstein, *Acta Crystallogr. Sect. B* **31**, 1268 (1975).
- ²³J. A. Bouwstra, A. Schouten, and J. Kroon, *Acta Crystallogr. Sect. C* **40**, 428 (1984).
- ²⁴L. H. Spangler, R. D. van Zee, and T. S. Zwier, *J. Phys. Chem.* **91**, 2782 (1987); L. H. Spangler, R. D. van Zee, S. C. Blankespoor, and T. S. Zwier, *ibid.* **91**, 6077 (1987).
- ²⁵T. Suzuki, N. Mikani, and M. Ito, *J. Chem. Phys.* **90**, 6431 (1986).
- ²⁶J. H. Simpson, N. Egger, M. A. Masse, D. M. Rice, and F. E. Karasz, *J. Polym. Sci.* **B28**, 1859 (1990); J. H. Simpson, D. M. Rice, and F. E. Karasz, *Polymer* **32**, 2340 (1991).
- ²⁷D. Chen, M. J. Winokur, M. A. Masse, and F. E. Karasz, *Polymer* **33**, 3116 (1992).
- ²⁸S. R. Bondeson and Z. G. Soos, *J. Chem. Phys.* **71**, 3807 (1979); **73**, 598 (1980); O. J. Heilmann and E. H. Lieb, *Trans. N.Y. Acad. Sci. Ser. II* **33**, 116 (1971).
- ²⁹M. Walczak and G. Stucky, *J. Am. Chem. Soc.* **98**, 5531 (1976).
- ³⁰T. Ikeyama and T. Azumi, *J. Phys. Chem.* **89**, 5332 (1985).
- ³¹B. Roos and P. N. Skancke, *Acta Chem. Scand.* **21**, 233 (1967); K. Schulten, I. Ohmine, and M. Karplus, *J. Chem. Phys.* **64**, 4422 (1976); O. Chalvet, J. Hoarau, J. Joussot-Dubien, and J. C. Rayez, *J. Chim. Phys.* **69**, 630 (1972); H. Labhart and G. Wagniere, *Helv. Chim. Acta* **46**, 1314 (1967).
- ³²S. Ramasesha and Z. G. Soos, *Int. J. Quantum Chem.* **25**, 1003 (1984); *J. Chem. Phys.* **80**, 3278 (1984); *Phys. Rev. B* **29**, 5410 (1984).
- ³³B. S. Hudson, B. E. Kohler, and K. Schulten, in *Excited States*, edited by E. Lim (Academic, New York, 1982), Vol. 6, p. 1.
- ³⁴P. Tavan and K. Schulten, *J. Chem. Phys.* **70**, 5407 (1979).
- ³⁵K. Ohno, *Theor. Chim. Acta* **2**, 219 (1964).
- ³⁶C. H. Ting and D. S. McClure, *J. Chin. Chem. Soc. (Taipei)* **18**, 95 (1971).
- ³⁷H. C. Longuet-Higgins and J. N. Murrell, *Proc. Phys. Soc. London* **A68**, 601 (1955).
- ³⁸G. Orlandi, P. Palmieri, and G. Poggi, *J. Am. Chem. Soc.* **101**, 3492 (1979).
- ³⁹R. R. Birge and B. M. Pierce, *J. Phys. Chem.* **70**, 165 (1979).
- ⁴⁰Z. G. Soos and S. Ramasesha, *J. Chem. Phys.* **90**, 1067 (1989); **92**, 5166 (1990).
- ⁴¹P. C. M. McWilliams, G. W. Hayder, and Z. G. Soos, *Phys. Rev. B* **43**, 9777 (1991).
- ⁴²J. A. Syage, P. M. Felker, and A. H. Zewail, *J. Chem. Phys.* **81**, 4706 (1984).
- ⁴³T. S. Zwier, E. M. Carrasquillo, and D. H. Levy, *J. Chem. Phys.* **78**, 5493 (1983).
- ⁴⁴Z. G. Soos and G. W. Hayden, *Phys. Rev. B* **40**, 3081 (1989).
- ⁴⁵S. Ramasesha and Z. G. Soos, *Chem. Phys.* **91**, 35 (1984).
- ⁴⁶H. Suzuki, *Bull. Chem. Soc. Jpn* **33**, 381 (1960).
- ⁴⁷A. L. Maniero and C. Corvaja, *Chem. Phys.* **135**, 277 (1989); T. Ikeyama and T. Azumi, *J. Phys. Chem.* **92**, 1383 (1988); G. Agostini, C. Corvaja, G. Giacometti, L. Pasimeni, and D. A. Clemente, *ibid.* **92**, 997 (1988).
- ⁴⁸W. G. Herkstroeter and D. S. McClure, *J. Am. Chem. Soc.* **90**, 4522 (1968).
- ⁴⁹H. Suzuki, K. Koyano, and T. L. Kunii, *Bull. Chem. Soc. Jpn* **45**, 1979 (1972).
- ⁵⁰C. A. Coulson, *Proc. R. Soc. London* **A169**, 413 (1939).
- ⁵¹H. C. Longuet-Higgins and L. Salem, *Proc. R. Soc. London Ser. A* **251**, 172 (1959); C. A. Coulson and A. Golebiewski, *Proc. Phys. Soc. London* **78**, 1310 (1961); M. J. S. Dewar and H. N. Schmeising, *Tetrahedron* **11**, 96 (1960).
- ⁵²D. Vanderbilt and E. J. Mele, *Phys. Rev. B* **22**, 3939 (1980).
- ⁵³L. Smilowitz and A. J. Heeger, *Synth. Met.* **48**, 193 (1992).
- ⁵⁴H. M. McConnell and D. B. Chesnut, *J. Chem. Phys.* **27**, 984 (1957); M. W. Hanna, A. D. McLachlan, H. H. Dearman, and H. M. McConnell, *ibid.* **37**, 361 (1962); A. Carrington, *Q. Rev. Chem. Soc.* **17**, 67 (1963).
- ⁵⁵Z. G. Soos and S. Ramasesha, *Phys. Rev. Lett.* **51**, 2374 (1983).
- ⁵⁶D. S. Galvão (unpublished).
- ⁵⁷E. Pellegrin, J. Fink, J. H. F. Martens, D. D. C. Bradley, H. Murata, S. Tokito, T. Tsutsui, and S. Saito, *Synth. Met.* **41**, 1353 (1991).
- ⁵⁸Z. G. Soos and G. W. Hayden, *Chem. Phys.* **143**, 199 (1990).
- ⁵⁹R. D. Miller and J. Michl, *Chem. Rev.* **89**, 1359 (1989).